

Strain-induced modulation of near-field radiative transfer

Alok Ghanekar,¹ Matthew Ricci,² Yanpei Tian,¹ Otto Gregory,² and Yi Zheng^{1,a)}

¹*Department of Mechanical, Industrial and Systems Engineering, University of Rhode Island, Kingston, Rhode Island 02881, USA*

²*Department of Chemical Engineering, University of Rhode Island, Kingston, Rhode Island 02881, USA*

(Received 24 April 2018; accepted 3 June 2018; published online 14 June 2018)

In this theoretical study, we present a near-field thermal modulator that exhibits change in radiative heat transfer when subjected to mechanical stress/strain. The device has two terminals at different temperatures separated by vacuum: one fixed and one stretchable. The stretchable side contains one-dimensional grating. When subjected to mechanical strain, the effective optical properties of the stretchable side are affected upon deformation of the grating. This results in modulation of surface waves across the interfaces influencing near-field radiative heat transfer. We show that for a separation of 100 nm, it is possible to achieve 25% change in radiative heat transfer for a strain of 10%. *Published by AIP Publishing.* <https://doi.org/10.1063/1.5037468>

The idea of thermal modulation, manipulation, and rectification has gathered significant attention in the past two decades. Conduction (phonons) based as well as radiation (photons) based thermal analogues of electronic devices such as thermal diodes,^{1,2} thermal transistors,^{3–5} thermal logic gates,⁶ and thermal memory elements⁷ have been presented in several research articles. The topic of heat manipulation is important due to its potential applications in thermal management, information processing,^{7–9} and energy conversion systems.

Due to the presence of Kapitza resistances and speed of phonons, phonon-based devices have some limitations.¹⁰ As a result, modulation of radiative heat transfer has become more attractive in recent years. Moreover, a radiation based device can take advantage of near-field effects—a regime where radiative heat transfer exceeds the blackbody limit by several orders of magnitude and attains heat modulation via manipulation of surface waves across the vacuum gap. Modulation of radiative heat transfer can be achieved by changing the distance between the substrates. Alternatively, manipulation of heat flux can be achieved by changing the optical properties of the materials and this approach is being investigated quite extensively. The principle idea of such devices is to utilize a change in optical properties of a phase-transition material to achieve a contrast in heat transfer.¹¹ For example, Zwol *et al.*¹² theoretically demonstrated a modulation of near-field radiative heat flux at a distance of 100 nm utilizing in crystalline and amorphous states of AIST (an alloy of silver, indium, antimony, and tellurium) that can be achieved using a current pulse. Yang *et al.*¹³ proposed a VO₂ based near-field radiative device that acts like a thermal switch. Numerous studies that rely upon enhancement or suppression of surface waves across the near-field gap to influence heat transfer can be found in the literature.^{13–18}

One of the shortcomings of phase-transition based heat modulation devices is that they must be operated around a particular temperature, such as 68 °C for VO₂. In the case of materials like silicon carbide, only a gradual heat modulation

is observed as the phase transition is not abrupt at a unique temperature. In contrast to work investigating phase-transition materials, work relating to heat modulation upon change in geometrical or mechanical configuration is sparse. Most notably, Biehs *et al.*¹⁹ showed that modulation of near-field heat transfer across two gratings can be attained by changing the relative orientation. In another instance, Liu *et al.*²⁰ presented a rotation-based near-field radiative thermal modulator that utilizes van der Waals materials. A key feature of such devices is that a continuous heat modulation is possible as opposed to thermal rectifiers that rely on phase transition.

The use of metamaterials to attain active control of optical properties, wavelength selective absorption, and emission has been researched before such as controlling optical properties through injection of electrical charge.²¹ Reconfigurable metamaterials have paved the way for dynamic control of optical and radiative properties.^{22,23} Moridani *et al.* demonstrated a tunable plasmonic thermal emitter using an elastically deformable plasmonic microstructure. Lee *et al.*²⁴ achieved dynamic control of thermal radiation by utilizing a foldable metamaterial. Such stretchable or foldable metamaterials can have a variety of applications in optoelectronic and biological sensors. These works deal with far-field configurations. However, such concepts have not yet been discussed in the near-field regime. In this letter, we investigate near-field radiative transfer between a planar structure and a grating-based microstructure wherein the grating-based structure is stretchable when subjected to mechanical stress. Here, the stretchable grating is the active metamaterial. We show that, it is possible to obtain a strong sensitivity of near-field radiative transfer to the mechanical strain.

Figure 1(a) introduces the concept of the near-field thermal modulator discussed here. In its simplest form, the device consists of two structures held at two different temperatures separated by a vacuum gap smaller than the wavelength of thermal radiation. Near-field radiative heat transfer between nanostructures has been measured before, and such configurations can be attained using mechanical spacers.^{25–27} One structure is made up of fixed planar media, while the

^{a)}Electronic mail: zheng@uri.edu

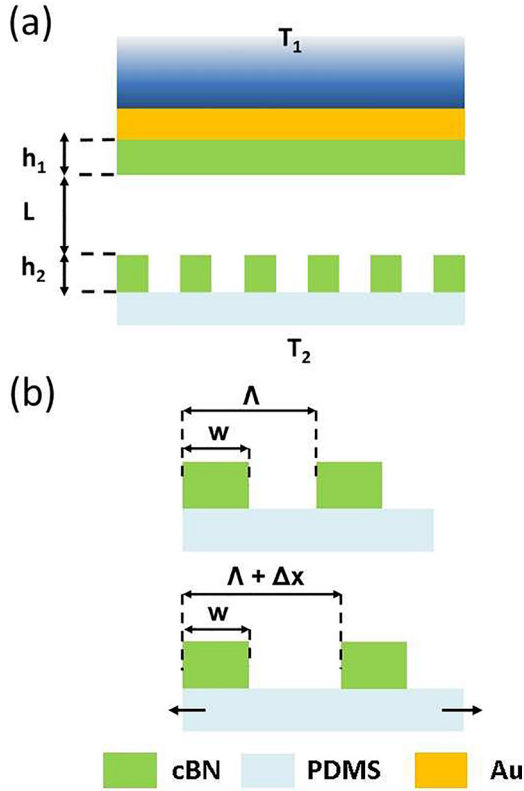


FIG. 1. Schematic of a near-field thermal modulator. (a) The fixed side has a thin film on cBN on a layer of gold while the stretchable side has 1-D rectangular grating of cBN on a layer of PDMS deposited on gold. (b) When the grating is stretched, the PDMS layer gets elongated along with the substrate, but cBN does not.

other has a stretchable grating that forms active or reconfigurable metamaterials. We propose to utilize a 1-D rectangular grating of a material over a thin film of an elastomer on the stretchable side. For simplicity, the choice of materials should be such that the grating material has a much higher Young's modulus than the polymer. To quantify thermal modulation, strain sensitivity α of such a thermal modulator can be defined as the ratio of relative change in heat transfer to the strain

$$\alpha = \frac{|\Delta Q|/Q}{\epsilon}. \quad (1)$$

Here, Q is the radiative heat flux across the interfaces in the neutral configuration with dimension x and $|\Delta Q|$ is the absolute change in heat transfer when subjected to mechanical strain of $\epsilon = |\Delta x|/x$. A schematic of the device upon mechanical strain is depicted in Fig. 1(b). In its neutral state, the grating has period Λ and filling ratio ϕ . The width of the grating material is $w = \Lambda\phi$. When subjected to a mechanical deformation of Δx , the polymer between the grating strips stretches and the grating period and the filling ratio change. The grating strip does not undergo any deformation as it has a much higher Young's modulus. It is also assumed that the part of the polymer layer right below the grating strip does not elongate. Therefore, the new grating period is $\Lambda + \Delta x$ and the new filling ratio is $w/(\Lambda + \Delta x)$. In this study, the stretchable side has a grating of cubic Boron Nitride over a 60 nm layer of Polydimethylsiloxane (PDMS). The fixed side has a layer of cBN over a $1 \mu\text{m}$ layer of gold deposited

on a substrate. The thickness of the cBN film h_1 , grating height h_2 , and neutral filling ratio ϕ can be tuned to achieve the maximum sensitivity of near-field radiative transfer to mechanical strain. Temperatures of the fixed side and stretchable side are assumed to be $T_1 = 301 \text{ K}$ and $T_2 = 300 \text{ K}$, respectively. The vacuum gap is assumed to be $L = 100 \text{ nm}$. Note that, when the grating is deformed, the thickness of the PDMS is also reduced. Owing to Poisson's ratio of PDMS (0.5), it is assumed that this change is negligible for the sake of simplicity. For example, a 10% strain leads to about 3 nm reduction in the total thickness of the PDMS layer. Furthermore, it is assumed that the separation between the two sides remains the same during deformation as it is maintained by mechanical spacers. Owing to the high elasticity of PDMS, it is assumed that the bonding between cBN strips and PDMS would not fail. From a practical consideration, this problem can be resolved by using an adhesive layer between cBN strips and PDMS. Since the majority of contribution to the radiative heat transfer is due to surface modes of cBN, the presence of the adhesive layer would not have a significant effect on the results. It is also assumed that the optical properties of PDMS do not change when subjected to mechanical deformation.

A potential fabrication scheme for the stretchable side of the proposed device can be achieved by fabrication of the cBN grating on a carrier substrate and that can be then transferred to the PDMS substrate via the "peel and stick" method. cBN grating can be deposited using chemical vapor deposition (CVD) and reactive etching on a carrier metal.²⁸ The grating can be delaminated using adhesive heat tape²⁹ and can be transferred to the final PDMS substrate.

The expression to calculate heat flux across the near-field thermal modulator can be obtained through dyadic Green's function formalism.³⁰ Radiative transfer between planar objects can be calculated by the following expression:

$$Q_{1 \rightarrow 2}(T_1, T_2, L) = \int_0^\infty \frac{d\omega}{2\pi} [\Theta(\omega, T_1) - \Theta(\omega, T_2)] T_{1 \rightarrow 2}(\omega, L), \quad (2)$$

where $\Theta(\omega, T) = (\hbar\omega/2) \coth(\hbar\omega/2k_B T)$ is the energy of the harmonic oscillator at frequency ω and temperature T , \hbar is the reduced Planck constant, and k_B is the Boltzmann constant. The function $T_{1 \rightarrow 2}(\omega, L)$ is called as the spectral transmissivity of radiative transport between media 1 and 2 separated by distance L ³⁰ and is expressed as

$$T_{1 \rightarrow 2}(\omega) = \int_0^\infty \frac{k_\rho dk_\rho}{2\pi} \xi(\omega, k_\rho). \quad (3)$$

Here, k_ρ is the parallel component of wavevector and $\xi(\omega, k_\rho)$ is known as the energy transmission coefficient and is given by

$$\begin{aligned} \xi(\omega, k_\rho \leq \omega/c) \\ = \sum_{\mu=s,p} \frac{(1 - |\tilde{R}_1^{(\mu)}|^2 - |\tilde{T}_1^{(\mu)}|^2)(1 - |\tilde{R}_2^{(\mu)}|^2 - |\tilde{T}_2^{(\mu)}|^2)}{|1 - \tilde{R}_1^{(\mu)} \tilde{R}_2^{(\mu)} e^{2jk_z L}|^2}, \end{aligned} \quad (4a)$$

$$\zeta(\omega, k_\rho > \omega/c) = \sum_{\mu=s,p} \frac{4\Re(\tilde{R}_1^{(\mu)})\Re(\tilde{R}_2^{(\mu)})e^{-2|k_z|L}}{|1 - \tilde{R}_1^{(\mu)}\tilde{R}_2^{(\mu)}e^{-2|k_z|L}|^2}, \quad (4b)$$

where $\tilde{R}_1^{(\mu)}$, $\tilde{R}_2^{(\mu)}$ and $\tilde{T}_1^{(\mu)}$ and $\tilde{T}_2^{(\mu)}$ are the polarized reflection and transmission coefficients of the two half spaces, $\mu = s$ (or p) refers to the transverse electric (or magnetic) polarization, and k_z is the z -component of wavevector in vacuum. $k_\rho \leq \omega/c$ and $k_\rho > \omega/c$ correspond to the propagating and evanescent modes, respectively. The expression is valid for multi-layered planar structures or planar media with effective dielectric properties. As our designs involve a 1-D grating structure of cBN in vacuum, second order approximation of effective medium theory was used to obtain the effective dielectric properties given by³¹

$$\varepsilon_{TE,2} = \varepsilon_{TE,0} \left[1 + \frac{\pi^2}{3} \left(\frac{\Lambda}{\lambda} \right)^2 \phi^2 (1 - \phi)^2 \frac{(\varepsilon_A - \varepsilon_B)^2}{\varepsilon_{TE,0}} \right], \quad (5a)$$

$$\varepsilon_{TM,2} = \varepsilon_{TM,0} \left[1 + \frac{\pi^2}{3} \left(\frac{\Lambda}{\lambda} \right)^2 \phi^2 (1 - \phi)^2 \times (\varepsilon_A - \varepsilon_B)^2 \varepsilon_{TE,0} \left(\frac{\varepsilon_{TM,0}}{\varepsilon_A \varepsilon_B} \right)^2 \right], \quad (5b)$$

where ε_A and ε_B are the dielectric functions of the two materials (cBN and vacuum) in surface gratings, λ is the wavelength, Λ is the grating period, and filling ratio $\phi = w/\Lambda$, where w is the width of the cBN segment. The expressions for zeroth order effective dielectric functions $\varepsilon_{TE,0}$ and $\varepsilon_{TM,0}$ are given by^{31,32}

$$\varepsilon_{TE,0} = \phi \varepsilon_A + (1 - \phi) \varepsilon_B, \quad (6a)$$

$$\varepsilon_{TM,0} = \left(\frac{\phi}{\varepsilon_A} + \frac{1 - \phi}{\varepsilon_B} \right)^{-1}. \quad (6b)$$

We limit ourselves within the domain of validity of the effective medium approximation (EMA) and choose grating period $\Lambda = 30$ nm that is much smaller than the thermal wavelength $\sim 10 \mu\text{m}$ at 300 K. Furthermore, the grating period must be smaller than the vacuum gap for the EMA to be valid for a near-field configuration.³³ $\Lambda = 30$ nm satisfies that criterion as well.

The dielectric properties of gold can be found in the study by Johnson and Christy.³⁴ Refractive indices of PDMS are taken from the study by Querry *et al.*,³⁵ while the dielectric function for cBN is taken from the study by Eremets *et al.*³⁶

Before reaching the choice of materials and configurations, numerical simulations were conducted for a variety of materials (including Si, SiO₂, ZnO, SiC, and gold) for the grating and the top layer of the fixed side. It was found out that, sensitivity is high when the same material is used on the stretchable side and the fixed side. As discussed later, the majority of near-field heat transfer is due to surface phonon polaritons and stronger coupling of surface waves is achieved when the same material is used on both the sides. Furthermore, it was observed that the choice of polymer and its layer thickness at the bottom of the grating is more or less irrelevant in the near-field regime. Hence, the PDMS layer

was fixed to 60 nm. This was followed by running an optimization routine for variables h_1 , h_2 , and ϕ to maximize α . Of the variety of structures and materials considered, the optimal configuration has cBN with $h_1 = 196$ nm, $h_2 = 150$ nm, and initial filling ratio $\phi = 0.6$.

In order to highlight strain-induced thermal modulation performance of the proposed device, Fig. 2(a) plots near-field radiative heat transfer across the device as a function of strain on the stretchable side. As can be clearly seen, the radiative heat flux drops with mechanical deformation of the grating. In the neutral position, radiative heat transfer across the device is about 35.7 W/m². When subjected to 5% strain, the filling ratio of the grating on the stretchable side changes from 0.6 to 0.54. As a consequence, radiative heat flux is reduced by $\sim 13\%$ to 26.7 W/m². This decrease is almost linear in this region, and the sensitivity (α) of this configuration is about 2.8. 10% deformation leads to $\sim 25\%$ reduction in heat flux; however, the trend is no longer linear. Larger deformation induces greater reduction in heat flux. Near-field heat transfer is reduced by 41% for 20% strain. At this point, the filling ratio of the cBN grating would be 0.5. To analyze the thermal modulation effect for gap spacing,

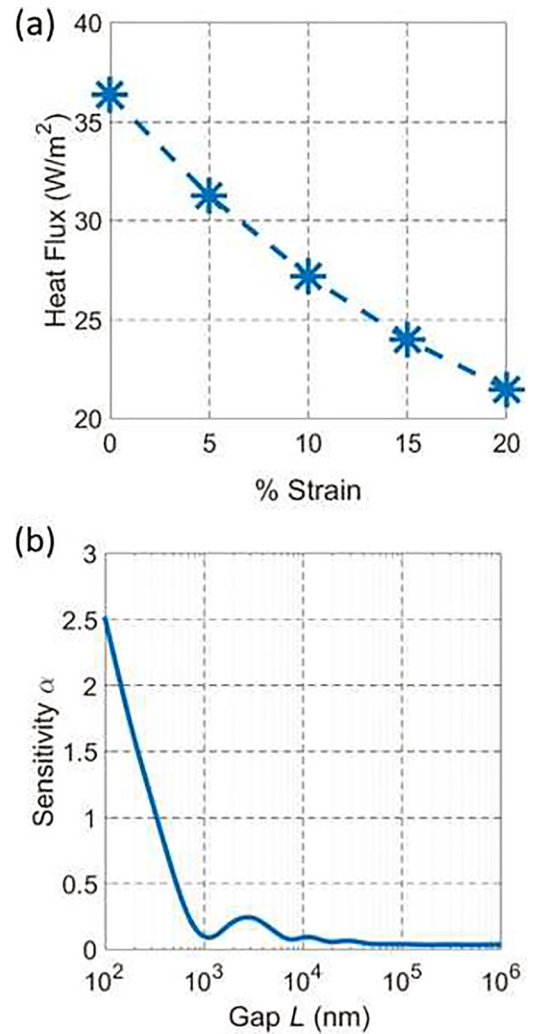


FIG. 2. (a) Strain dependent heat flux shown for the optimal configuration of thermal modulator. 10% strain on the stretchable side causes nearly 25% reduction in the heat transfer. (b) Sensitivity of the proposed device as a function of separation between the structures.

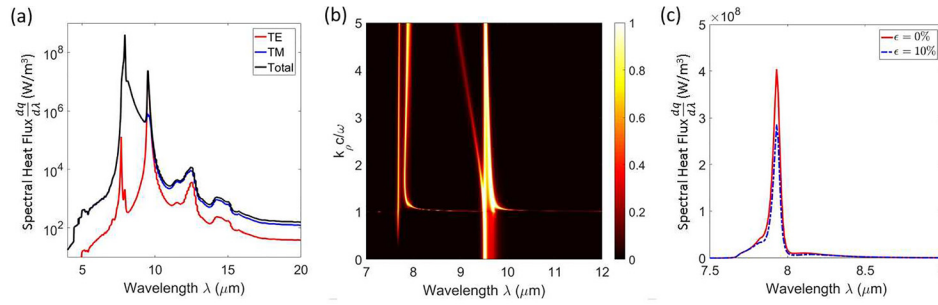


Fig. 3. (a) Spectral heat flux in neutral configuration ($\epsilon = 0\%$) of the proposed device, contributions of TE and TM polarizations are shown. (b) Coefficient of energy transmission $\xi(\omega, k_{\rho})$ across the two interfaces of thermal modulator in neutral configuration plotted against wavelength and normalized parallel wave vector $k_{\rho}c/\omega$. (c) TM component of spectral heat flux in neutral vs 10% strained configuration.

Fig. 2(b) plots the sensitivity of the device against the gap. Sensitivity drops dramatically as the distance is increased and becomes near constant for gaps larger than $\sim 1 \mu\text{m}$. As contribution of surface waves is negligible in the far-field, the structures are relatively insensitive to strain or a small change in the filling ratio.

Figure 3(a) shows spectral radiative heat flux across the interfaces of the proposed thermal modulator without deformation of the stretchable side. The total spectral heat flux and contributions of TE and TM modes are shown. The two sharp peaks seen in the spectral plot correspond to the frustrated modes of cBN. These are the characteristic wavelengths of cBN ($7.6 \mu\text{m}$ and $9.8 \mu\text{m}$). Since cBN supports surface phonon polaritons (SPhPs), near-field radiative heat transfer can be attributed to symmetric and anti-symmetric surface phonons. It can be clearly observed that the contribution of the TE mode is practically negligible when compared to the overall heat transfer. Moreover, the majority of the spectral heat flux is centered around $7.6 \mu\text{m}$ where the dielectric function of cBN becomes negative and refers to surface phonon polariton dispersion. Figure 3(b) depicts the coefficient of energy transmission across the interfaces against normalized parallel wave vector ($k_{\rho}c/\omega$) and wavelength. The bright regions of the plot show high transmission that occurs near $7.6 \mu\text{m}$ and $9.8 \mu\text{m}$. High transmission at large values of normalized parallel wave vector ($k_{\rho}c/\omega \gg 1$) at these wavelengths suggests dominant contribution of surface phonon polaritons. There exists a weak contribution due to Fabry-Perot modes and frustrated modes ($k_{\rho}c/\omega \approx 1$) in the near-field regime. Spectral heat flux due to the TM mode for 0% and 10% strain is plotted in Fig. 3(c). When subjected to the strain of 10%, a reduction in spectral heat flux is seen near $\lambda \sim 7.6 \mu\text{m}$, the wavelength at which the coupling of SPhPs occurs, while the rest of the spectrum is relatively unchanged. This peak, however, occurs at the same location $\lambda = 7.92 \mu\text{m}$ with and without deformation. Strain-induced change in the filling ratio resulting in the change in the effective optical properties of the grating layer disturbs the coupling of SPhPs across the interfaces. The lower filling ratio is believed to be causing an increased scattering of surface waves leading to weaker coupling of surface modes. Therefore, materials supporting surface polaritons are more suitable for the proposed concept.

While we limit ourselves to the analysis of the design with a 60 nm thick PDMS layer, it is possible to use thicker layers of PDMS. From the analytical point of view, one of

the challenges of such a design is that, when such a layer is deformed, its thickness changes by a non-negligible amount. Furthermore, owing to the rigidity of cBN, the thickness of the PDMS layer between the grating strips and that below the grating strip will be different, leading to a non-uniform deformation of the PDMS layer. A more detailed simulation of the structure is necessary to analyze deformation of such a structure. However, a key advantage of such a design is that, when deformed, the separation between the two sides of the modulator also changes (increases). These changes can be quite significant for thicker layers of PDMS. It would lead to an increased sensitivity of the device. We leave this point to be addressed in future works. We would like to highlight that a negative strain or compression of the grating side would have a similar effect on near-field radiative heat flux. To address the issue of buckling of the grating structure during compression, one can design the device with pretension in the PDMS layer. Negative strain in such a scenario will then be feasible, and the device would be sensitive to both tensile and compressive strains.

Thus, we have presented a concept of a near-field thermal modulator that exhibits sensitivity to subjected mechanical strain to modulate radiative heat transfer. A grating of cBN on a polymer layer of PDMS allows reversible stretching of the structure. Deformation of the grating leads to a change in the filling ratio of the grating, and therefore, the effective optical properties of the grating layer can be actively changed. In the proposed design, the deformation causes a reduced coupling of surface waves across the interfaces and reduces the near-field heat flux across the vacuum gap. In the optimal configuration, 10% deformation can cause about 25% change in radiative heat transfer. Given the elastic properties of PDMS, greater modulation of heat flux is possible for larger deformation. Moreover, the device can be made sensitive to negative strains by having pretension in the PDMS layer. A further increase in sensitivity can be attained by using thicker layers of PDMS. The proposed device allows dynamic and reversible control of radiative transfer. Such concepts can be explored for negative index metamaterials and hyperbolic metamaterials. It has potential applications in near-field strain gauges, optoelectronic devices, and biological sensors and actuators.

This project was supported in part by National Science Foundation through Grant No. 1655221, Institutional Development Award (IDeA) Network for Biomedical

Research Excellence from the National Institute of General Medical Sciences of the National Institutes of Health under Grant No. P20GM103430, and Rhode Island Foundation Research Grant No. 20164342.

- ¹B. Li, L. Wang, and G. Casati, "Thermal diode: Rectification of heat flux," *Phys. Rev. Lett.* **93**, 184301 (2004).
- ²P. Ben-Abdallah and S.-A. Biehs, "Phase-change radiative thermal diode," *Appl. Phys. Lett.* **103**, 191907 (2013).
- ³B. Li, L. Wang, and G. Casati, "Negative differential thermal resistance and thermal transistor," *Appl. Phys. Lett.* **88**, 143501 (2006).
- ⁴A. Ghanekar, Y. Tian, M. Ricci, S. Zhang, O. Gregory, and Y. Zheng, "Near-field thermal rectification devices using phase change periodic nanostructure," *Opt. Express* **26**, A209–A218 (2018).
- ⁵P. Ben-Abdallah and S.-A. Biehs, "Near-field thermal transistor," *Phys. Rev. Lett.* **112**, 044301 (2014).
- ⁶L. Wang and B. Li, "Thermal logic gates: Computation with phonons," *Phys. Rev. Lett.* **99**, 177208 (2007).
- ⁷N. Li, J. Ren, L. Wang, G. Zhang, P. Hänggi, and B. Li, "Colloquium: Phononics: Manipulating heat flow with electronic analogs and beyond," *Rev. Mod. Phys.* **84**, 1045 (2012).
- ⁸P. Ben-Abdallah and S.-A. Biehs, "Towards Boolean operations with thermal photons," *Phys. Rev. B* **94**, 241401 (2016).
- ⁹V. Kubyskiy, S.-A. Biehs, and P. Ben-Abdallah, "Radiative bistability and thermal memory," *Phys. Rev. Lett.* **113**, 074301 (2014).
- ¹⁰P. Ben-Abdallah and S.-A. Biehs, "Contactless heat flux control with photonic devices," *AIP Adv.* **5**, 053502 (2015).
- ¹¹A. Ghanekar, J. Ji, and Y. Zheng, "High-rectification near-field thermal diode using phase change periodic nanostructure," *Appl. Phys. Lett.* **109**, 123106 (2016).
- ¹²P. Van Zwol, K. Joulain, P. Ben-Abdallah, J.-J. Greffet, and J. Chevrier, "Fast nanoscale heat-flux modulation with phase-change materials," *Phys. Rev. B* **83**, 201404 (2011).
- ¹³Y. Yang, S. Basu, and L. Wang, "Vacuum thermal switch made of phase transition materials considering thin film and substrate effects," *J. Quant. Spectrosc. Radiat. Transfer* **158**, 69–77 (2015).
- ¹⁴Y. Yang, S. Basu, and L. Wang, "Radiation-based near-field thermal rectification with phase transition materials," *Appl. Phys. Lett.* **103**, 163101 (2013).
- ¹⁵J. Huang, Q. Li, Z. Zheng, and Y. Xuan, "Thermal rectification based on thermochromic materials," *Int. J. Heat Mass Transfer* **67**, 575–580 (2013).
- ¹⁶A. Ghanekar, G. Xiao, and Y. Zheng, "High contrast far-field radiative thermal diode," *Sci. Rep.* **7**, 6339 (2017).
- ¹⁷P. Van Zwol, L. Ranno, and J. Chevrier, "Tuning near field radiative heat flux through surface excitations with a metal insulator transition," *Phys. Rev. Lett.* **108**, 234301 (2012).
- ¹⁸F. Menges, M. Dittberner, L. Novotny, D. Passarello, S. Parkin, M. Spieser, H. Riel, and B. Gotsmann, "Thermal radiative near field transport between vanadium dioxide and silicon oxide across the metal insulator transition," *Appl. Phys. Lett.* **108**, 171904 (2016).
- ¹⁹S.-A. Biehs, F. S. Rosa, and P. Ben-Abdallah, "Modulation of near-field heat transfer between two gratings," *Appl. Phys. Lett.* **98**, 243102 (2011).
- ²⁰X. Liu, J. Shen, and Y. Xuan, "Pattern-free thermal modulator via thermal radiation between van der Waals materials," *J. Quant. Spectrosc. Radiat. Transfer* **200**, 100–107 (2017).
- ²¹T. Inoue, M. De Zoysa, T. Asano, and S. Noda, "Realization of dynamic thermal emission control," *Nat. Mater.* **13**, 928 (2014).
- ²²I. M. Pryce, K. Aydin, Y. A. Kelaita, R. M. Briggs, and H. A. Atwater, "Highly strained compliant optical metamaterials with large frequency tunability," *Nano Lett.* **10**, 4222–4227 (2010).
- ²³I. M. Pryce, Y. A. Kelaita, K. Aydin, and H. A. Atwater, "Compliant metamaterials for resonantly enhanced infrared absorption spectroscopy and refractive index sensing," *ACS Nano* **5**, 8167–8174 (2011).
- ²⁴S. Lee, S. Kim, T.-T. Kim, Y. Kim, M. Choi, S. H. Lee, J.-Y. Kim, and B. Min, "Reversibly stretchable and tunable terahertz metamaterials with wrinkled layouts," *Adv. Mater.* **24**, 3491–3497 (2012).
- ²⁵R. S. DiMatteo, P. Greiff, S. L. Finberg, K. A. Young-Waithe, H. Choy, M. M. Masaki, and C. G. Fonstad, "Enhanced photogeneration of carriers in a semiconductor via coupling across a nonisothermal nanoscale vacuum gap," *Appl. Phys. Lett.* **79**, 1894–1896 (2001).
- ²⁶L. Hu, A. Narayanaswamy, X. Chen, and G. Chen, "Near-field thermal radiation between two closely spaced glass plates exceeding Planck's blackbody radiation law," *Appl. Phys. Lett.* **92**, 133106 (2008).
- ²⁷K. Ito, A. Miura, H. Iizuka, and H. Toshiyoshi, "Parallel-plate submicron gap formed by micromachined low-density pillars for near-field radiative heat transfer," *Appl. Phys. Lett.* **106**, 083504 (2015).
- ²⁸A. Werbowy, J. Szmids, A. Sokołowska, and S. Mitura, "RF plasma selective etching of boron nitride films," *Diamond Relat. Mater.* **9**, 609–613 (2000).
- ²⁹C. H. Lee, D. R. Kim, and X. Zheng, "Transfer printing methods for flexible thin film solar cells: Basic concepts and working principles," *ACS Nano* **8**, 8746–8756 (2014).
- ³⁰A. Narayanaswamy and Y. Zheng, "A Green's function formalism of energy and momentum transfer in fluctuational electrodynamics," *J. Quant. Spectrosc. Radiat. Transfer* **132**, 12–21 (2014).
- ³¹D. H. Raguin and G. M. Morris, "Antireflection structured surfaces for the infrared spectral region," *Appl. Opt.* **32**, 1154–1167 (1993).
- ³²E. Glytsis and T. K. Gaylord, "High-spatial-frequency binary and multi-level staircase gratings: Polarization-selective mirrors and broadband anti-reflection surfaces," *Appl. Opt.* **31**, 4459–4470 (1992).
- ³³X. Liu, T. Bright, and Z. Zhang, "Application conditions of effective medium theory in near-field radiative heat transfer between multilayered metamaterials," *J. Heat Transfer* **136**, 092703 (2014).
- ³⁴P. B. Johnson and R.-W. Christy, "Optical constants of the noble metals," *Phys. Rev. B* **6**, 4370 (1972).
- ³⁵M. Querry, "Optical constants of minerals and other materials from the millimeter to the UV," U.S. Army Report No. CRDEC-CR-88009, Aberdeen, MD, 1987.
- ³⁶M. Eremets, M. Gauthier, A. Polian, J. Chervin, J. Besson, G. Dubitskii, and Y. Y. Semenova, "Optical properties of cubic boron nitride," *Phys. Rev. B* **52**, 8854 (1995).